JOURNAL OF MATERIALS SCIENCE: MATERIALS IN MEDICINE 2 (1991) 162–167

Ultrastructural study of the effects of coral skeleton on cultured human gingival fibroblasts in three-dimensional collagen lattices

A. H. M. SHABANA*, J. P. OUHAYOUN*, H. BOULEKBACHE‡, J. M. SAUTIER*, N. FOREST*
Laboratoire de Biologie-Odontologie, ‡Laboratoire de Biologie du Developpement, Universite Paris 7, France

Natural coral skeleton has recently been introduced as a bone graft substitute which enhances bone formation in man and animals. The effects of NCS on cultured human cells has not previously been investigated. In the present study we report these effects as studied by light microscopy, transmission and scanning electron microscopy in three-dimensional culture. The results showed that natural coral skeleton does not inhibit the normal function of fibroblasts in contracting collagen lattices. After 8 weeks, the cells maintained a healthy ultrastructural morphology. At the collagen/coral interface, the cells were well-spread and attached to the surface by numerous adhesion plaques. Evidence for biosynthetic activity was also observed; the cells showed numerous ribosomes, mitochondria and prominent rough endoplasmic reticulum. Extracellularly, a perigranular dense matrix, appearing as nodules in the SEM, was deposited on the coral surface. This matrix was made of highly organized fibrils lacking periodicity, and a ground substance. The present study shows that coral was well-tolerated by human gingival fibroblasts, and that it provided a surface for cell spreading, attachment and deposition of the special extracellular matrix.

1. Introduction

Several alloplastic implants have been used as bone graft replacements in bone defects and to augment the alveolar bone. Most of these materials have been calcium phosphate ceramics in the form of tricalcium phosphate or hydroxyapatites, and variable results have been obtained regarding the effects of these materials on bone formation [1–7]. Natural coral skeleton (NCS) of genus porites, as reported previously [8, 9] is made of 98% calcium carbonate in the form of aragonite crystals, 1% amino acids and 0.005% heavy metals. The skeleton is porous with an average pore diameter of 150 μm. Experimental studies in animals [8, 9] and in man [10–12] have shown that NCS enhances bone formation; the material is resorbed gradually and is replaced during new bone formation. In alveolar bony defects prepared in the mandibles of pigs, coral granules were covered by osteoid tissue and the defects were progressively closed by well-formed bone [13]. Human periodontal defects implanted with NCS showed reduction of pocket depth and enhancement of bone formation [14]. The present authors reported that coral was clinically well-tolerated and histologically did not stimulate immune reactions [13, 14]. To date, however, the *in vitro* effects of coral on human cells have not been reported. The purpose of the present study is to examine by light, scanning (SEM) and transmission (TEM) elecron microscopy the effects of NCS on cultured human gingival fibroblasts in order to gain further insight into the cell–coral interactions and *in vitro* aspects of biocompatibility of the material. In the present study we used three-dimensional collagen lattices for culture. This culture system allowed the study of an important aspect of fibroblast function, that is to contract collagen, and to observe the behaviour of cells in three-dimensional space around the material.

2. Materials and methods

2.1. Culture

Gingival tissues were obtained during extraction of impacted teeth from young patients (15–30 years). The tissues were washed three times in Earl's modified Eagle's culture medium (EMEM), supplemented with 100 IU ml^{-1} penicillin, 100 μg ml^{-1} streptomycin, 2.5 μg ml^{-1} amphotericin and 10% fetal calf serum. Fibroblast primary cultures were established from 1 mm^3 tissue explants. The tissue dishes were kept at 37 °C in a humid atmosphere containing 5% CO_2. Confluent fourth passage cells were harvested by using 0.05% trypsin in 0.02% EDTA at 37 °C for 10 min. Trypsin was inactivated by 10% fetal calf serum in the culture medium and the cells were washed and suspended as 2×10^5 ml^{-1} in EMEM ready to be used for collagen lattices preparation.

Collagen lattices containing fibroblasts were prepared in 60 mm-diameter petri dishes by methods described previously [15]. For each lattice, 4.6 ml concentrated (×1.7) EMEM containing antibiotics,

0022–2461/91 $03.00 + .12

0.9 ml fetal calf serum, 3.0 ml of 2 mg ml^{-1} collagen solution (extracted from rat's tail tendon by 0.1% acetic acid and stored at 4 °C), 0.5 ml of 0.1 N NaOH, and 1.0 ml fibroblast suspension were mixed at 4 °C and reversed in the petri dishes. Before collagen polymerization at 37 °C, NCS in the form of 300–450 μm granules was added to 15 lattices as 10 mg per lattice. Ten other lattices were prepared as described above and left without coral incorporation (controls). Cultures were fed twice a week with EMEM containing antibiotics and fetal calf serum as described above for 56 days.

During the culture period, collagen lattice diameter was measured on millimeter graph paper. After 56 days, the contracted lattices were treated by conventional methods for light and electron microscopy. At least three lattices from each group were processed for each type of microscopic investigation.

2.2. Tissue processing

For light microscopy, lattices were fixed in 10% formol saline, decalcified in 5% nitric acid for 24 h, dehydrated in ethanol solutions, 50, 70, 90 and 100%, for 10 min in each dilution. The tissue was then embedded in paraffin wax and tissue blocks were cut into 5 μm-thick sections. Deparaffinized sections were stained with haematoxylin and eosin.

For ultrastructural studies the lattices were washed in 0.1 M sodium cacodylate buffer containing 0.1 M sucrose (pH 7.4), fixed for 30 min in 2% glutraldehyde in the washing buffer, and post-fixed for 15 min in 0.5% osmium tetroxide and 0.8% potassium ferrocyanide in cacodylate buffer. After washing, the tissues were further processed for either TEM or SEM. Tissue blocks for TEM were treated in 0.15% tannic acid for 1 min to enhance collagen staining, then washed. The tissues were stained with 2% uranyl acetate in 50% ethanol for 40 min, then dehydrated in ethanol solutions and propylene oxide, Epon–Araldite thin sections were stained with lead citrate solution (1.76 g lead citrate and 1.83 g lead nitrate in 50 ml H_2O) for 30 min and examined with Philips 400 electron microscope.

Tissues for SEM were dehydrated in increasing concentrations of ethanol and in 100% isoamyl–acetate prior to critical point drying from CO_2. The blocks were fractured and coated with 30 nm gold in a Polaron sputtering apparatus. Specimens were then examined with a Jeol JSM-35 microscope at 15 or 25 kV.

3. Results

3.1. Phase contrast microscopic observations

During the first 2 weeks, collagen was semi-transparent and it was possible to observe the cell behaviour inside. At the time of seeding, the cells were rounded and uniformly distributed in the collagen. Three hours later, the cells showed extended cytoplasmic processes in the three-dimensional space made by the lattices. There was neither apparent orientation nor arrangement of cells. Within 5 days, it became clear that the cells near the coral had changed in their orientation; the cell long axis became parallel to the coral surface. Other cells appeared to attach to the coral. These observations could not be followed up after day 14 due to the increasing density of the contracting lattices.

Collagen contraction started by the following day of lattice preparation (original diameter = 53 mm). A state of stability was achieved after 4 weeks. Changes in lattice diameter over 8 weeks in culture, in the presence and absence of coral, are shown in Fig. 1. The average diameter became smaller in coral-incorporated lattices as early as the third day and reached maximum on day 7. The differences, however, were not statistically significant using two-tailed t-test ($p > 0.05$) indicating that coral incorporation does not alter fibroblast function in contracting the lattices. During the following 3 weeks, stronger contraction in the controls reduced the difference between the two groups.

3.2. Light microscopic observations

Decalcified paraffin sections and undecalcified semithin sections of the lattices showed the same features. In the controls (absence of coral), collagen fibres and fibroblasts were randomly distributed in the tissue. Some cells were present on the external surfaces of the lattices. These were flattened and sometimes formed a continuous layer. In coral-incorporated lattices, similar features were observed. However, in the vicinity of coral, fibroblasts were elongated with their long axis parallel to the surface of the coral. Other fibroblasts were present at the collagen/coral interface, and appeared to attach to the material. Around some granules, fibroblasts were present in a dense collagenous matrix (Fig. 2).

3.3. Electron microscopic findings

Ultrastructural examination of undecalcified thin sections showed that the cells maintained a healthy

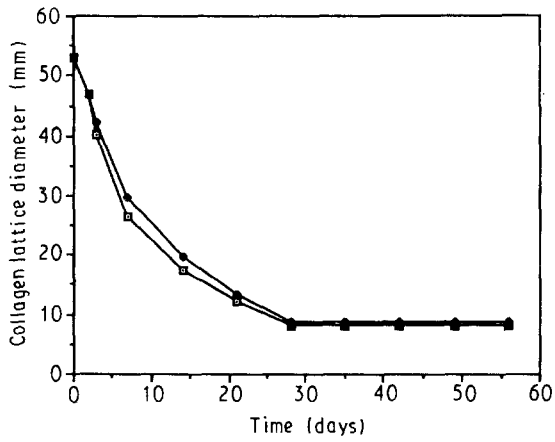

Figure 1 Collagen contraction by human gingival fibroblasts in the presence and (□) absence (●) of coral. Strong contraction occurred during the first 7 days. Following this active phase, collagen contraction gradually decreased to the 28th day; no more contraction occurred up to the 56th day. The differences observed in the presence and absence of coral were statistically insignificant ($p > 0.05$).

morphology typical of fibroblasts; the abundance of mitochondria, prominent rough endoplasmic reticulum, few empty lysosomes and procollagen-like material. The shape of the nucleus generally followed the shape of the cell (Fig. 3). The cells in the lattices were stellate-shaped with cytoplasmic processes extending in various directions. Those at the surface were flattened, long, spindle-shaped cells with short cytoplasmic processes. Newly formed collagen was differentiated from the collagen of the lattices by its smaller diameter (40 against 70 nm) and by being more electron dense (Fig. 4), and was found in larger quantities at the borders of the lattices.

In the SEM, the collagen lattice appeared as a network of fibres between which fibroblasts were dispersed. Coral granules showed two distinct topographies, a fractured coral surface made of 1×100 μm prismic aragonite crystals and an external unfractured surface. The cells were preferentially attached to the latter surface and were found to penetrate the pores of coral. In coral-incorporated lattices, mineral crystals of varying sizes were found within and on the surfaces of the lattices.

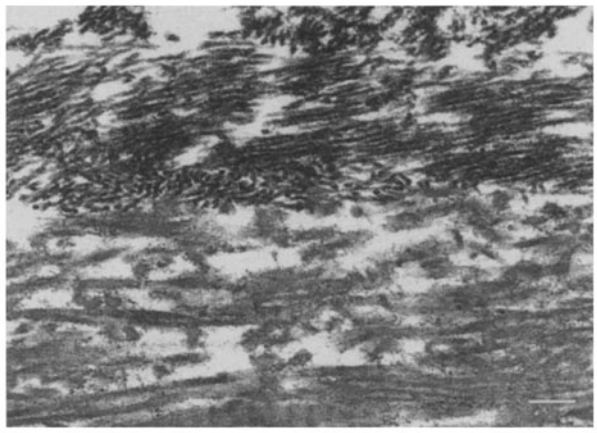

Figure 4 New collagen synthesis occurred at the external surface of the lattices. The new collagen (top) differs from that of the lattice (bottom) by being more organized, thinner in cross section (40 nm) and more electron dense. TEM, scale bar = 500 nm.

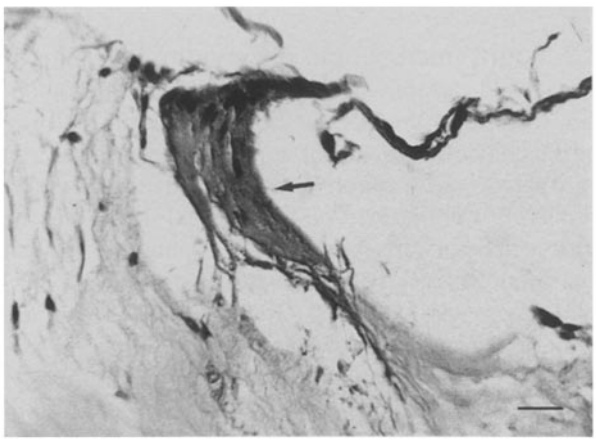

Figure 2 Decalcified paraffin section of a 56-day lattice incorporated with coral. A newly formed dense matrix (arrow) is directly deposited at the coral/collagen interface. The collagen of the lattice (left) appears less dense and the fibroblasts are randomly distributed. Some cells are also present at the surface of the lattice and lining the space left by decalcified coral. Haematoxylin and eosin stain, scale bar = 15 μm.

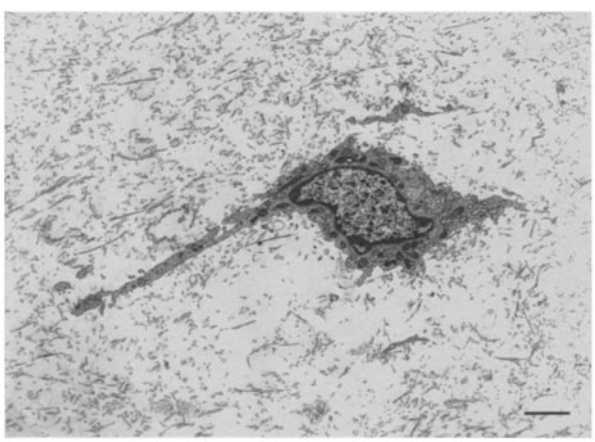

Figure 3 The human gingival fibroblasts in the coral-incorporated lattices maintained healthy ultrastructural morphology. One typical stellate-shaped fibroblast with numerous mitochondria, some vesicles, rough endoplasmic reticulum, Golgi apparatus and ribosomes. The cytoplasmic processes extend in various directions and attach to the surrounding collagen fibres. No specific orientation of the fibres is seen. TEM, scale bar = 2 μm.

The cells at the coral/collagen interface were well spread indicating good attachment, and were of two phenotypes: the first, and more common, was of typical extremely elongated spindle-shaped fibroblasts (Fig. 5); and the second, less common, was of disc-shaped cells with central nucleus (Fig. 6). Cell attachment occurred through numerous adhesion plaques distributed alongside the cell membrane, through filopodia and cytoplasmic processes. These were more numerous and longer at the polar ends of the cells (see Fig. 5, inset). At the rough surface of the coral, cell attachment occurred through these filopodia and cell processes, which formed multipoints of attachment, and a wide gap between the cell and the material gave a relief effect (Figs 5 and 7). At the smooth surface, this gap was hardly distinguishable below the well-spread and flattened cells (see Fig. 5 inset and Fig. 6). In the TEM this was sometimes as small as 15 nm. At the coral/collagen interface the cells also formed solid nodular structures around which collagen sheets and cells were found (Fig. 8).

In the TEM, these cells showed well-developed rough endoplasmic reticulum and numerous attached and free ribosomes in the cytoplasm. Procollagen-like material and a cytoskeletal network of microfilaments were prominent features. Membrane-bound vesicles containing electron-dense amorphous material were present in these cells. The vesicles were well rounded or oval-shaped, 500 nm in diameter, and were associated with the cell side facing the newly formed matrix (Fig. 9). The extracellular matrix was made of highly organized newly formed fibrils of 4–6 nm in diameter, oriented parallel to the long axis of the cells. These fibrils lacked periodicity, and formed bundles that crossed each other at sharp angles. Within this fibrillar matrix, electron-dense amorphous material resembling the contents of the membrane bound vesicles was found (Fig. 10). These morphological features indicated high biosynthetic activity.

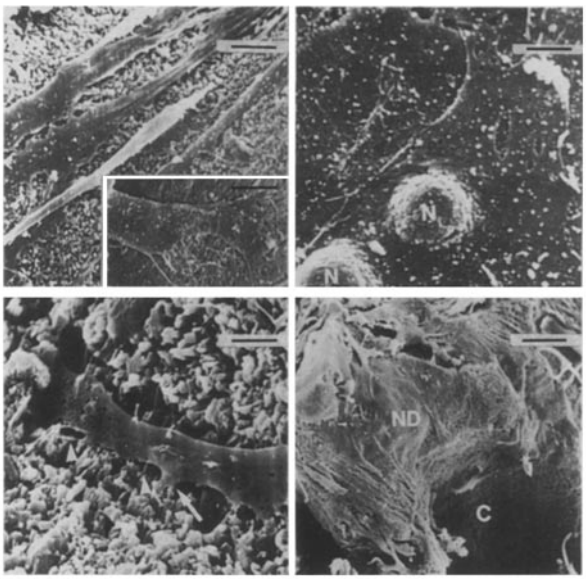

Figure 5 Fibroblasts attached to coral were extremely elongated and flattened spindle-shaped cells. The figure shows four of these cells attached to coral rough surface through filopodia. Note the large gap between coral and the cell body. SEM, scale bar = 3.3 μm. The inset shows one polar end of a cell which is well-spread, and numerous processes attaching it to a smooth coral surface. No gap between the material and the cell can be observed. SEM, scale bar = 2.8 μm.

Figure 6 Less often, another cell phenotype was found to attach to coral. This was an extremely flattened disc-shaped cell with central nucleus (N). The cells spread and attached to coral with no obvious gap. SEM, scale bar = 1.7 μm.

Figure 7 Part of a cell located in a small groove on the fractured surface of coral. Filopodia (arrow) and processes (arrow heads) extended in various directions and attached to coral crystals. A few cells were present on such a surface (compare with Fig. 8) and little if any collagen matrix was deposited. SEM, scale bar = 1.25 μm.

Figure 8 On the external unfractured coral surface (C) numerous cells were attached and a new matrix was deposited around the cells. The figure shows a nodular structure (ND) and the associated cells. This surface is relatively smooth (compare with Fig. 7) as seen in the lower right side which corresponds to a part of a pore. SEM, scale bar = 5 μm.

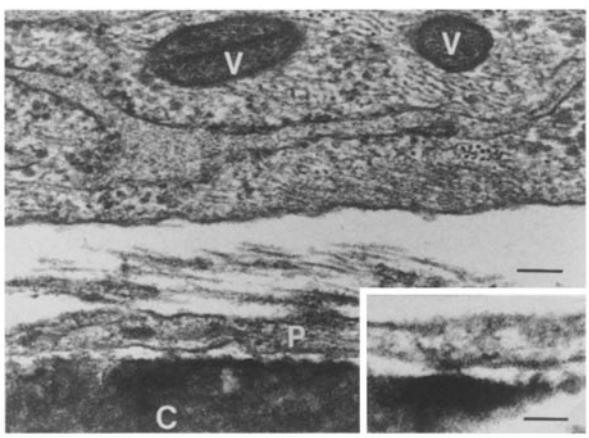

Figure 9 Cell attachment to coral. At the coral/matrix interface, a multilayer of cells was found. In the middle, a cytoplasmic process extends directly on the coral surface (C) and attaches to it by numerous adhesion plaques. Inset, high magnification of one adhesion plaque (scale bar = 36 nm). An extracellular matrix made of fine fibrils and ground substance is deposited between a cell (top) and a cell process (P). The cell shows prominent rough endoplasmic reticulum, numerous free and attached ribosomes, and microfilaments. Membrane-bound vesicles (V) containing electron-dense amorphous material are shown. TEM, scale bar = 128 nm.

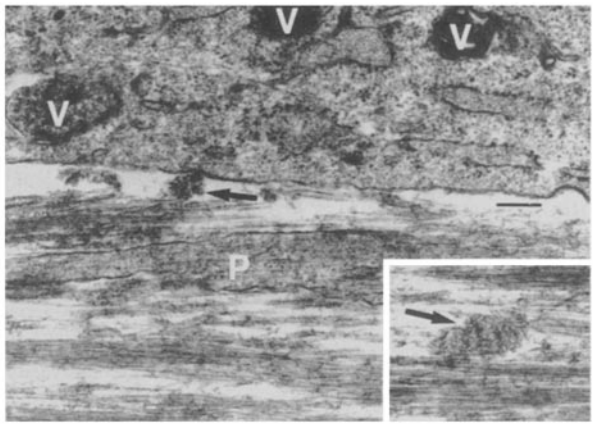

Figure 10 The ultrastructure of the newly formed matrix at the coral/lattice interface. The matrix is made of 5 nm fibrils arranged parallel to each other, and forming bundles that cross each other at sharp angles. The orientation of the bundles follows the plane of cell spreading. Within this matrix, a material resembling the contents of the membrane-bound vesicles (V) was found. The extracellular electron-dense amorphous material (arrows), also shown in the inset, has similar size to that of the vesicles. TEM, both figure and inset at same magnification, scale bar = 500 nm.

4. Discussion

One of the normal functions of fibroblasts in culture is to contract collagen lattices. It has previously been shown that collagen contraction is related to cell mobility [16], and the integrity of actin mirofilaments [15–18]. During the first week in culture, we observed cell mobility around the coral granules and attachment to the surface which explains the slight enhancement of collagen contraction. Ultrastructurally, these cells show prominent cytoskeletal microfilaments that correspond to actin. Other factors controlling the degree of contraction include cell number, age and origin, in addition to the incubation temperature, the density of collagen, the quantity of serum and some mediators of cell growth and differentiation such as retinoids and hormones [19–21]. Cytotoxic agents such as chlorhexidine acetate and anthraquinone glycoside inhibit collagen contraction [22–24]. Thus collagen contraction by fibroblasts can be useful for testing cytotoxicity of various materials, including implant materials. In the present long-term culture, coral incorporation did not inhibit the contractile function of human gingival fibroblasts, and the cells maintained healthy ultrastructural features, even those in the immediate vicinity of the coral. These findings demonstrate the absence of a cytotoxic effect of coral on human gingival fibroblasts.

In vivo, contraction is believed to play a role in certain biological processes such as contraction of wounds, and a specialized cell designated as a myofibroblast was held responsible for scar formation [25, 26]. *In vitro*, several cell types can contract collagen gels including fibroblasts, rat calvaria cells and epithelial rests of Malassez [27], thus there is no justifiable relation between *in vivo* scar formation and *in vitro* collagen contraction. When a low-energy implant material which does not allow for cell attachment is used, a fibrous capsule develops all around the material [28]. In the present study, we show in culture

direct evidence of cell spreading and attachment on the coral surface, and capsule formation is not found in this study or in previous *in vivo* studies [13, 14, 29].

At the surface of the collagen lattice, the cells were flattened and a new matrix made of collagen and ground substance was deposited. This is in contrast with a scarce deposition within the lattices. These observations were reported previously [30–35] and are not associated with the presence or absence of coral. These authors explained inhibition of collagen synthesis within the lattices by the inhibitory effect of collagen binding to the cell membrane: cells cultured on collagen attach by one side only. Another explanation implicates cell shape – fibroblasts cultured on plastic or on collagen assume a flattened morphology and show high biosynthetic activity, whereas those cultured in collagen assume a stellate shape and show low biosynthetic activity [28, 36–38].

In the present study, new matrix formation was detected both around coral (in collagen) and on the lattice surfaces. In both sites the cells were long and spindle-shaped. These findings suggest that the effect of cell shape on biosynthesis is more important than the effect of collagen binding to the cell membrane. The new matrix on the surfaces of the lattices was made of 40 μm-wide collagen fibres with periodicity. In contrast, the matrix formed on coral surfaces was made of 5 μm-wide fibrils lacking periodicity. Furthermore, the cells at the coral/collagen interface were extremely flattened and elongated. These differences suggest an effect of coral on the cell to deposit a special matrix. Coral skeleton contains 98% calcium carbonate, 1% amino acids and traces of heavy metals. Arginine, glycine and aspartic acid exist amongst the amino acids. It is interesting to note that these three polypeptides are shared by all cell attachment molecules such as fibronectin, laminin, vitronectin and epibolin [29]. It is not surprising to find excellent attachment throughout the two month period in culture. These adhesion molecules in addition to the other amino acids may also have contributed to the induction of the dense perigranular matrix. In SEM, anchoring fibrillar structures were clearly seen extending between the cells and adjacent surface of coral. We suggest that these are fibronectin-rich fibrils which were detected by monoclonal antibodies (data not shown).

The present results also show that human gingival fibroblasts preferentially attach to the unfractured external surface of coral granules, rather than to the rough surface made by fractured aragonite crystals. These observations are in accordance with previous reports showing that mesenchymal cells attach to smooth surfaces and macrophages attach to rough surfaces [39]. It was also on the external surface of coral that we found deposition of a new matrix. On the rough surface, fibroblasts attached by filopodia and cell processes, with large gap between the cell and the material. In contrast, fibroblasts attached to smooth surfaces were well-spread, leaving practically no gap, thus indicating excellent attachment. Previous studies on the effects of coral on bone repair have shown conflicting results regarding phagocytic activity around the material [8, 9, 13, 40]. It is possible that the proportion of smooth to rough surfaces in the different size of granules used in these studies is responsible for this controversy.

In a previous study we reported the formation of perigranular calcification in the gingiva of pigs observed 3–6 months after coral implantation [41]. In the present study, mineral crystals were detected in lattices incorporated with coral. The deposition of mineral crystals in the lattices may occur without cell involvement, for example by the binding of calcium with phosphate in high ionic strength in culture medium [42]. However, the cells also exhibited membrane-bound vesicles containing electron-dense amorphous material resembling mineral crystals. The perigranular dense matrix appeared as nodular structures. This matrix shares features in common with early mineralizing tissues [43]. The associated cells were mainly flattened, spindle-shaped fibroblasts and some were disc-shaped cells. The role and type of the latter cells have to be ascertained. Reddi and Huggins [44] reported the sequences in the transformation of normal fibroblasts of rats to bone-forming cells when acid-insoluble bone matrix extracts were implanted subcutaneously. Further investigations are necessary to show if fibroblast transformation can occur following coral incorportion in *vitro*, and to characterize the nature of the perigranular dense matrix.

The present results show that coral does not alter the normal functions of fibroblasts in contracting collagen lattices and deposition of extracellular matrix. Ultrastructurally, no evidence of cytotoxicity was observed for coral in long-term culture. Finally, coral provided a surface for the attachment of human gingival fibroblasts and induced the deposition of a special perigranular matrix.

Acknowledgements

We are thankful for the technical assistance provided in cell culture by Mme N. Martin and in electron microscopy by Mmes M. Oboeuf and F. Meury, and for the secretarial assistance of Mme K. Marlin and Mr E. Marie-Rose.

References

1. M. L. RABALAIS, R. A. YUKNA and E. T. MAYER, *J. Periodontol.* **52** (1981) 680.
2. B. S. MOSKOW and A. LUBORR, *ibid.* **54** (1983) 455.
3. R. A. YUKNA, E. T. MAYER and O. V. BRITE, *ibid.* **55** (1984) 633.
4. R. A. YUKNA, B. G. HARRISON, R. F. CAUDILL, G. H. EVANS, E. T. MAYER and S. MILLER, *ibid.* **56** (1985) 540.
5. E. B. KENNEY, V. LEKOVIC, J. C. SA FERREIRA, T. HAN, B. DIMITRIJEVIC and A. CARRANZA Jr, *ibid.* **57** (1986) 76.
6. S. W. SAPKOS, *ibid.* **57** (1986) 7.
7. F. L. BYE, M. E. KRAUSE, S. A. REGEZI and R. G. CAFFESSE, *ibid.* **58** (1987) 110.
8. G. GUILLEMIN, J. L. PATAT, J. FOURNIÉ and M. CHETAIL, *J. Biomed. Mater. Res.* **21** (1987) 557.
9. G. GUILLEMIN, A. MEUNIER, P. DALLANT and P. CRISTEL, *ibid.* **23** (1989) 765.
10. A. PATEL, F. HONNAST, G GUILLEMIN and J. L. PATAT, *Chirurgie* **106** (1980) 199.

11. J. C. POULIQUEN, M. NOAT, C. VERNERET, G. GUILLEMIN and J. L. PATAT, *Revue de chirurgie orthopédique*, **75** (1989) 360.
12. Y. LEVET, S. GUERO, G. GUILLEMIN and G. JOST, *Ann. Chir. Plast. Esthét.* **33** (1988) 279.
13. J. P. OUHAYOUN, A. H. M. SHABANA, S. ISSAHAKIAN, J. L. PATAT, G. GUILLEMIN, M. H. SAWAF and N. FOREST, *J. Mater. Sci: Mater. in Med.* in press.
14. S. ISSAHAKIAN and J. P. OUHAYOUN, *J. Parodontol.* **8** (1989) 251.
15. E. BELL, B. IVARSSON and C. MERRILL, *Proc. natnl. Acad. Sci. USA* **76** (1979) 1274.
16. A. K. HARRIS, D. STOPAK and P. WILD, *Nature* **290** (1981) 249.
17. C. G. BELLOWS, A. H. MELCHER and J. E. AUBIN, *J. Cell Sci.* **58** (1982) 125.
18. D. J. BUTTLE and H. P. EHRLICH, *J. Cell Physiol.* **116** (1983) 159.
19. B. M. STEINBERG, K. SMITH, M. COLOZZO and R. POLLACK, *J. Cell Biol.* **87** (1980) 304.
20. L. W. ADAMS and G. C. PRIESTLEY, *J. Invest. Dermatol.* **87** (1986) 544.
21. B. COULOMB, Thèse (diplôme d'Etat), Université de Paris-sud, 1988.
22. Y. KUBOTA, K. FUJIWARA, I. OGATA, Y. HORI and H. OKA, *Brit. J. Dermatol.* **113** (1985) 559.
23. G. C. PRIESTLEY, *ibid.* **117** (1987) 67.
24. L. W. ADAMS and G. C. PRIESTLEY, *Arch. Dermatol. Res.* **280** (1988) 114.
25. T. ELSDALE and J. BARD, *J. Cell Biol.* **54** (1972) 626.
26. K. YOSHIZATO, T. TAIRA and N. YAMAMOTO, *J. Biomed. Res.* **6** (1985) 61.
27. C. G. BELLOWS, A. H. MELCHER and J. E. AUBIN, *J. Cell Sci.* **50** (1981) 299.
28. S. NAKAGAWA, P. PAWELEK and F. GRINNELL, *ibid.* **182** (1989) 572.
29. E. RUOSLAHTI and M. D. PIERSCHBACHER, *Science* **238** (1987) 491.
30. G. GABBIANI, C. CHAPONNIER and I. HUNTTNER, *J. Cell Biol.* **76** (1978) 561.
31. G. GABBIANI, B. J. HIRSCHEL, G. B. RYAN, P. R. STATKOV and G. MAJNO, *J. exp. Med.* **135** (1972) 719.
32. R. SARBER, B. HULL, C. MERRILL, T. SORANNO and E. BELL, *Mech. Ageing Devl.* **17** (1981) 107.
33. B. NUSGENS, C. MERRILL, C. LAPIERE and E. BELL, *Collagen Related Res.* **4** (1984) 351.
34. F. M. VAN BOCKXMEER, C. E. MARTIN and I. J. CONSTABLE, *Exp. Cell Res.* **155** (1984) 413.
35. M. BAYE, B. V. NUSGENS and C. M. LAPIÈRE, *Eur J. Cell Biol.* **45** (1987) 44.
36. E. N. UNEMORI and Z. WERB, *J. Cell Biol.* **103** (1986) 1021.
37. C. MAUCH, A. HATAMOCHI, K. SHORFETTER and T. KRIEG, *Exp. Cell Res.* **178** (1988) 493.
38. T. NISHIYAMA, M. TSUNENAGA, Y. NAKAYAMA, E. ADACHI and T. HAYASHI, *Matrix* **9** (1989) 193.
39. D. M. BRUNETTE, *Int. J. Oral Maxillofac. Implants* **3** (1988) 231.
40. M. HOTT, P. J. MARIE, G. GUILLEMIN and J. L. PATAT, in "Hybride Artificial Organ" edited by C. Baquey and B. Dubuy (Colloque INSERM, 1989) p. 311.
41. A. H. M. SHABANA, J. P. OUHAYOUN, J. L. PATAT and N. FOREST, *J. Dent. Res.* **68** (1989) 644.
42. G. K. HUNTER, S. C. NYBURG and K. P. H. PRITZKER, *Collagen Rel. Res.* **6** (1986) 229.
43. J-R. NEFFUSSI, M-L. LEFÈVRE, H. BOULEKBACHE and N. FOREST, *Differentiation* **29** (1985) 160.
44. A. H. REDDI and C. HUGGINS, *Proc. natnl. Acad. Sci. USA* **69** (1972) 1601.

Received 23 July
accepted 12 November 1990